WHEEL TRAFFIC EFFECT ON AIR-FILLED POROSITY AND AIR PERMEABILITY IN A SOIL CATENA ACROSS THE WHEEL RUT

Berisso F.E.[1], Schjønning P.[1], Lamandé M.[1], Weisskopf P.[2], Stettler M.[3], Keller T.[2,4]

[1]*Aarhus University, Denmark;* [2] *Agroscope Research Station ART, Switzerland;* [3] *Bern University of Applied Sciences, School of Agricultural, Forest and Food Sciences HAFL, Switzerland;* [4] *Swedish University of Agricultural Sciences, Sweden*

Abstract

The impact of wheel traffic on soil physical properties is usually quantified by randomly collecting soil cores at specific depths below the wheeled surface. However, modeling studies as well as few measurements indicated a non-uniform stress distribution in a catena across the wheel rut, which might induce different effects on soil physical properties. The objective of this study was to investigate the impact of vehicle traffic on soil physical properties and air permeability by systematic collection of samples in a transect running from the center to the outside of the wheel rut. A field experiment was conducted on a clay loam soil at Suberg, Switzerland, in 2010. Four repeated wheeling were performed by driving a forage harvester (wheel load of 6100 kg and a tyre width of 0.8 m) forward and rearward in the same track. We sampled 100 cm^3 intact cores at 10, 30 and 50 cm depth in a soil catena running from center of the wheel rut to un wheeled part of the field (0, 20, 40, 50,60 and 400 cm horizontal distance). We measured water retention and air permeability (k_a) at -30, -100 and -300 hPa matric potentials. At -100 hPa, we obtained consistently lower air filled under the wheel rut than at the periphery of the wheel rut (0.4 m) or outside the wheel rut. At least one of these differences ε_a was significant at all soil depths . At all matric potentials, the k_a was lowest at the periphery of the wheel rut and highest outside the wheel rut, with intermediate values inside the wheel rut. However significant differences in k_a were obtained only at 10 cm depth. The lowest air permeability at the periphery of the wheel rut is interpreted as a distortion of the soil pores due to shear strain rather than isotropic compaction. Our results indicate that sampling in the soil catena can provide better resolution on information about traffic induce changes on soil physical properties.

Keywords: Compaction, Shear stress, Soil catena, Air permeability, Air-filled porosity

Introduction

Nowadays there is a trend toward using heavier and efficient agricultural machinery in order to maximize the economic returns (reduce cost of production) from agricultural production unit. Use of heavy machinery, on the other hand, puts more stress on soil, which may result in undesirable soil conditions due to compaction. Changes on physical and mechanical properties due to field traffic had been reported in many studies (e.g. 1, 2, 3). These changes are usually quantified by randomly collecting soil cores at specific depths below the wheeled surface. This is similar to assuming that the vehicle pass would resulted in uniform changes in the soil physical properties (at any depth) within the wheel rut (soil-tyre contact area). In spite of these, it has long been since many modeling (4, 5, 6, 7) and measurement (8, 9, 10) studies indicating inhomogeneous stress distribution under vehicle wheels.

The objective of this study was to investigate the impact of vehicle traffic on soil physical properties and air permeability by systematic collection of samples in a transect running from the center to the outside of the wheel rut. This transect is termed ‘catena’ in this paper.

Material and Methods

Site description and field experiment

A soil compaction experiment was conducted in autumn 2010 on an arable filed at Suberg (47.06 °N, 7.33 °E) near Bern, Switzerland. The field has been grassland for four years and used for grazing, mainly by cattle. The upper 10-50 cm of soil has a clay-loam texture with clay and sand content ranging from 0.19 to 0.27 and 0.45 to 0.54 g g^{-1}, respectively. The soil organic matter content ranges from 0.01 to 0.024 g g^{-1}. The average particle densities *(PD)* of the soil are 2.58, 2.61 and 2.63 g cm^{-3} at 10, 30 and 50 cm depth, respectively.

The experiment had a randomized block design with four replicate plots and comprised five to six sampling positions in the soil catena running from the center of the wheel rut to the un wheeled part of the plots. The wheeled part of the plots were subjected to four repeated wheeling with an eight-row self-propelled forage harvester (the Claas make Jaguar 890 Field shuttle). A front axle of the harvester had a wheel load of 6000 and 6100 kg at the right and left sides, respectively. The tyre type was GoodYear DT (820, 800/65R32) and was inflated to a pressure of 200 kPa (recommend at speed of 30 km hr^{-1}: 190 kPa). Wheeling was done only with the front-right-side tyre in the same track by driving the harvester forward and rearward (forward-rearward-forward-rearward). The crab steering system of the harvester prevented an overlap between the tracks of the front and the rear wheels.

Soil sampling

After wheeling, an access pit with 200 x 200 x 100 cm (width x length x depth) was carefully opened at each plot and horizontal planes were sequentially prepared for sampling at 10, 30 and 50 cm depth. Intact cores of 100 cm^3 were collected at 0, 20, 40 , 50 and 300 cm horizontal distances from the centre of the wheel rut (perpendicular to the driving direction) and in the control plots at all three sampling depths. Additional cores were collected at 60 cm horizontal distance from the center of the wheel rut at 30 and 50 cm depth. At each sampling position, three replicate cores were collected for each combination of plots and sampling depths, which makes a total of 384 cores.

Laboratory analysis

Water retention and air permeability

Prior to laboratory analyses, the soil cores were carefully trimmed with a sharp-edged knife, covered with fine nylon cloth and placed in a trough, where the water saturated the soil cores from the bottom within 24 hours in three steps. Then the samples were kept in the water for a week and finally transferred to sandboxes, where they sequentially drained to -30, -100 and -300 hPa matric potentials.

The air permeability was measured by applying a pressurized air of 2 hPa on the top of core and the flow rate was automatically registered by data logger. After each measurement, the data was downloaded to the PC and the air permeability was calculated using Darcy's law.

After k_a measurement at -300 hPa, the cores were oven-dried at 105 ºC for 24 hours. Samples were weighed at each matric potential and after oven drying. Soil bulk density *(BD)* was calculated from the weight of the oven-dried soil and the total volume of the core. Total porosity (θ_s) was calculated from *BD* and *PD*. Gravimetric water content *(w)* was determined as the difference between the weight of the samples at a given matric potential and that the oven–dry weight. Volumetric water content at a given matric potential (θ) was calculated from *w* and *BD*. Air-filled porosity (ε_a) was determined as the difference between θ_s and θ.

Calculations

Pore continuity indices

Pore continuity indices of Suberg soil can be assessed by combining measurements of air-filled porosity and air permeability (at three matric potentials) as given by Ball et al. (10):

$$k_a = M\varepsilon_a^N \qquad (1)$$

where *M* and *N* are empirical parameters. The parameter '*N*' is regarded as pore continuity index that reflects an increase of k_a with increasing ε_a or the decrease of pore tortuosity with the increasing fraction of pores available for flow. Mostly, these parameters are determined by fitting a straight line in a log-log plot of k_a vs ε_a:

$$\log(k_a) = \log(M) + N\log(\varepsilon_a) \qquad (2)$$

We also evaluated a pore functional index at a given matric potentials from the ratio of k_a to ε_a. Blackwell et al. (12) referred to this index as "pore organization" (*PO*), which is given by:

$$PO = k_a / \varepsilon_a \qquad (3)$$

Statistics

Statistical analysis was performed with mixed procedure in SAS with horizontal positions as fixed effect and block and interaction between block and horizontal position as random effect using the following model:

y=μ + horizontal position + block + block × horizontal position

The Kenward and Roger (13) method was used for calculations of degrees of freedom. An autoregressive, AR(1), covariance structure was used to account for correlation between samples from the same plot at different horizontal positions.

Results and discussion

Air-filled porosity and air permeability at -100 hPa

After four repeated wheelings, ε_a at -100 hPa was generally lower under the wheel rut (0-20 cm horizontal distance from the center of the wheel rut) than at the periphery of the wheel rut (40 cm) or outside the wheel rut (50-300 cm horizontal distance from the center of the wheel rut) (Fig.1). This trend applied for soil at all depths, although the results were significant at 10 and 30 cm depth (at 50 cm depth, ε_a was higher for soil at 300 cm horizontal distance than for soils in a catena from the center of the wheel rut to 60 cm).

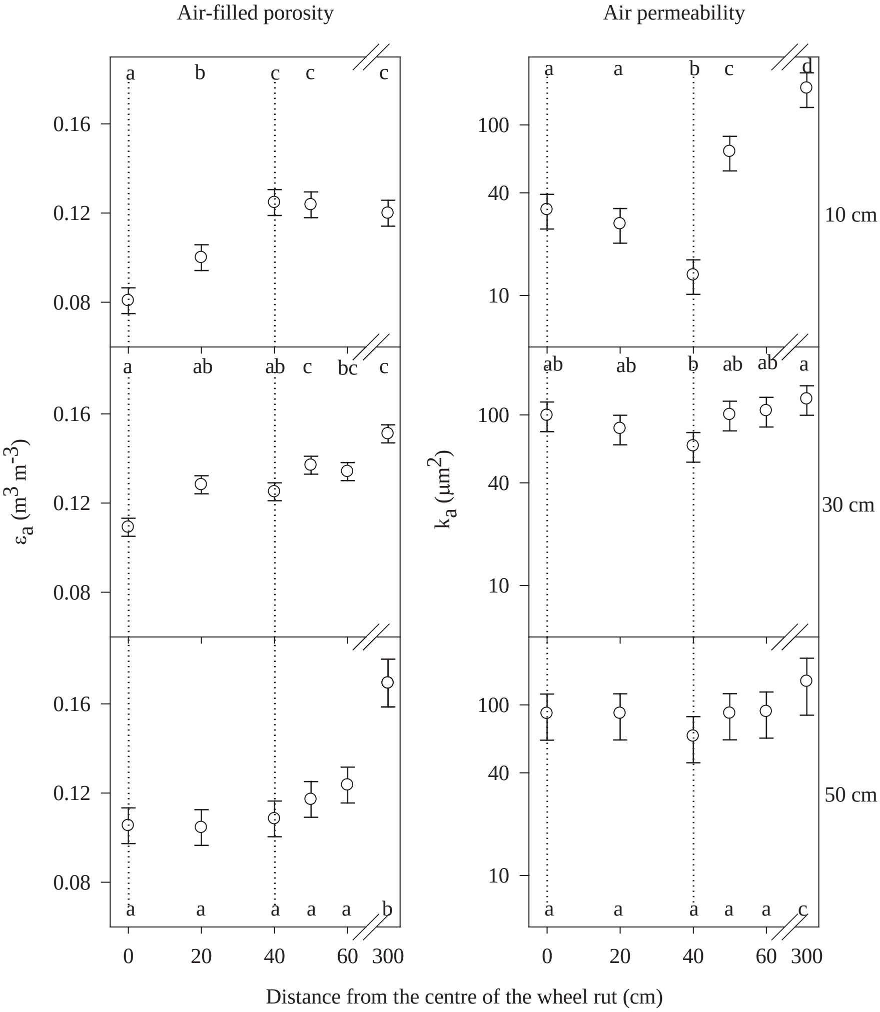

Figure 1. Air-filled porosity (left) and air permeability (right) measured at -100 hPa as a function of the horizontal distance from the center of the wheel rut at 10 cm (upper two figures), 30 cm (middle two figures) and 50 cm (lower two figures) depth. The dotted lines indicates the center and the periphery of the wheel rut.

Within the wheel rut, there were also differences in ε_a values in all three soil depths. However significant differences were observed only at 10 depth in the following order: ε_a was lowest at the center of the wheel rut and highest at the periphery of the wheel, with intermediate values at 20 cm from the center of wheel rut. This pattern of ε_a at this depth portrays the stress distribution pattern in the tyre-soil contact areas as proposed in several studies (4,6,9).

Air permeability at 30 and 50 cm soil depth showed a trend of reduction after four repeated wheeling; however, no significant compaction effect was observed except for the soil at the periphery of the wheel rut at 30 cm depth (Fig. 1). In contrast, we observed a significant compaction effect on k_a of soil 10 cm depth (Fig. 1). For soil at 10 cm depth, we also note that the wheeling effect on k_a depends on the horizontal distance from the center of the wheel rut: it was lower for soil at 50 cm horizontal distance from the center of the wheel rut than for soil under the wheel rut (at 0-20 cm horizontal distance from the center of wheel rut), which in turn is much lower than for soil at the periphery of the wheel rut. This means that k_a was lowest at periphery of wheel rut. However, at this horizontal distance, ε_a was not affected by compaction (Fig. 1). A possible mechanism to explain these observations can be a distortion of soil due to stress field at the periphery of the wheel rut. Distortion can affect the connectivity of vertical pores and thereby the associated convective gas transport.

Pore continuity indices

The log-log plots of k_a as a function of ε_a together with the regression lines (Eq. 2) for soil from all sampling depths at some selected horizontal distances from the center of wheel rut (0, 40 and 300 cm) are shown in Fig. 2. As expected, a strongly increasing linear (R^2 ranging from 0.84 to 0.99) and significant relationship (P values mostly < 0.001) was obtained between k_a and ε_a in log-log scale. Similar relationship have been reported in several studies (9, 14, 15, 16,17).

Soils at 10 cm depth under the wheel rut presented remarkable differences: the log k_a vs log ε_a plots for the soil at the centre and at the periphery of the wheel rut lie above and below similar plot for the soil at 300 cm horizontal distance from the center of the wheel rut, respectively (Fig. 2a). During wheeling, the soil at the center of the wheel rut is exposed to compressive forces that significantly reduced ε_a (for all three three matric potentials (-30, -100 and -300 hPa) and thereby k_a as shown in Fig 2a. However, there was no significant difference in *N* (the *N* parameter shows the rate of opening of continuous pore paths with decreasing matric potential) between the soils at the center of wheel rut and 300 cm horizontal distance from the center of the wheel rut. This could reflect the fact that the soil at the center of wheel rut was compressed equally from all sides (the pores were primarily reduced in size, but not destroyed). In contrast, the value of *N* for the soil at the periphery of the wheel rut was significantly higher than the value for the soil at 300 cm horizontal distance from the center of the wheel rut During wheeling, the pore network of soil at the periphery of the wheel rut might shear off and it could be blocked easily by water bridges. As the soil drains, these bridges disappear and continuous path-ways are open (the lines in Fig. 2 seem to converge with decreasing matric potential) . At the two lower depths (30 and 50 cm), no significant differences in the *N* parameter was observed.

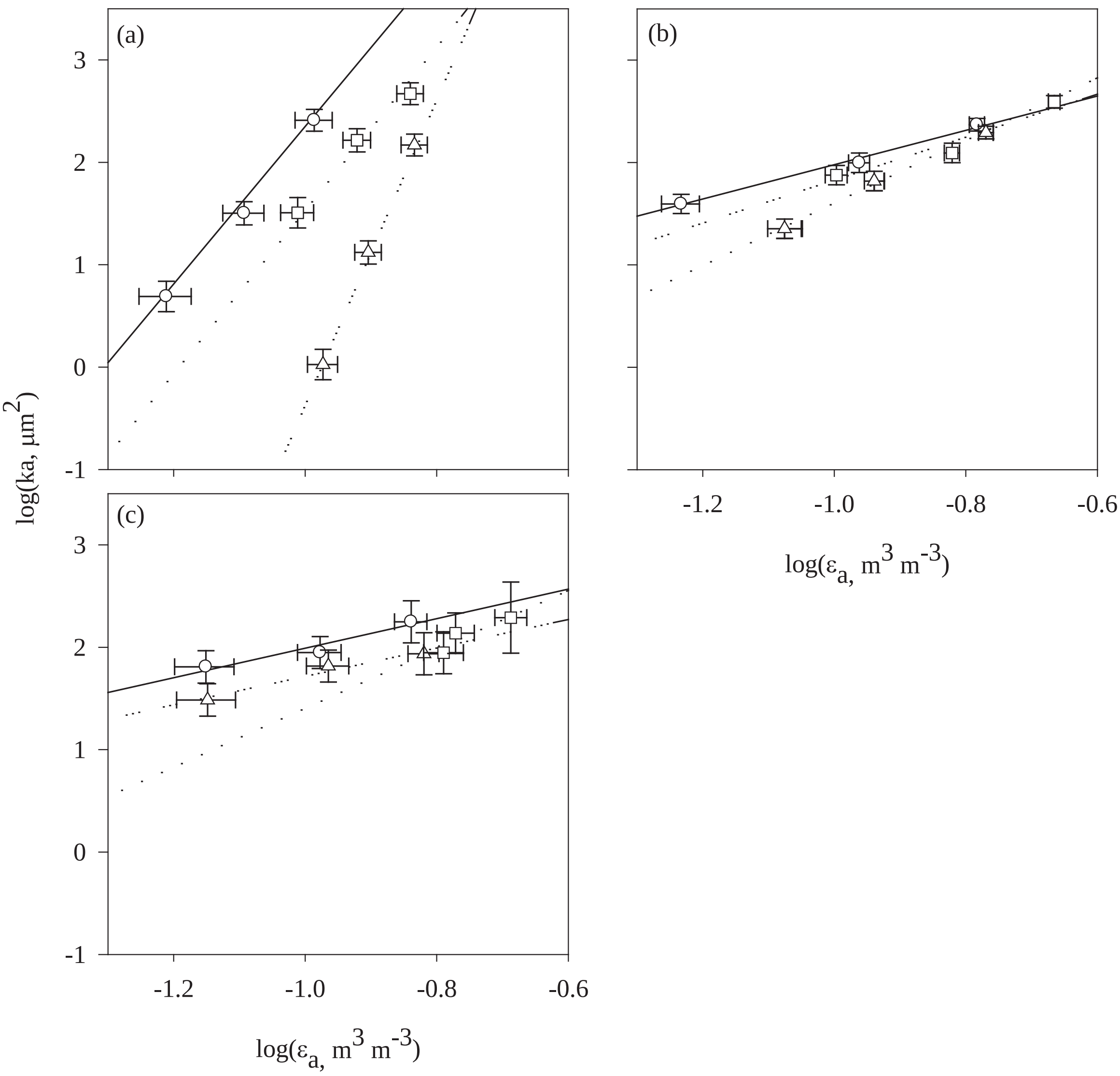

Figure 2. Relationship between air permeability and air filled porosity for Suberg soils sampled at the center (circle and solid line) and the periphery (triangle and short- dashed and dotted line) of the wheel rut, and control plot (square and short-dashed line) at 0.1 (a), 0.3(b), and 0.5 (c) m depths.

Pore organization as a function of ε_a is shown in Fig. 3 for soils at some selected horizontal distances from the center of the wheel rut (0,40 and 300 cm). Air permeability isolines (2.5, 25 and 250 μm^2) were also included to reinforce the trend observed in Fig. 2b-c. No significant differences in *PO* were observed at 30 and 50 cm depth (except at -30 hPa matric potential and at 30 cm depth, between soils at the periphery of the wheel rut and at 300 cm horizontal distance from the center of wheel rut; Fig 3b-c). In contrast, we found significant effects of compaction on *PO* at all three matric potentials at 10 cm depth: *PO* was greatest for the soil at 300 cm horizontal distance from the center of wheel rut and smallest for the soil at the periphery of the wheel rut, with intermediate values in the soil at the center of the wheel rut (Fig. 3a).

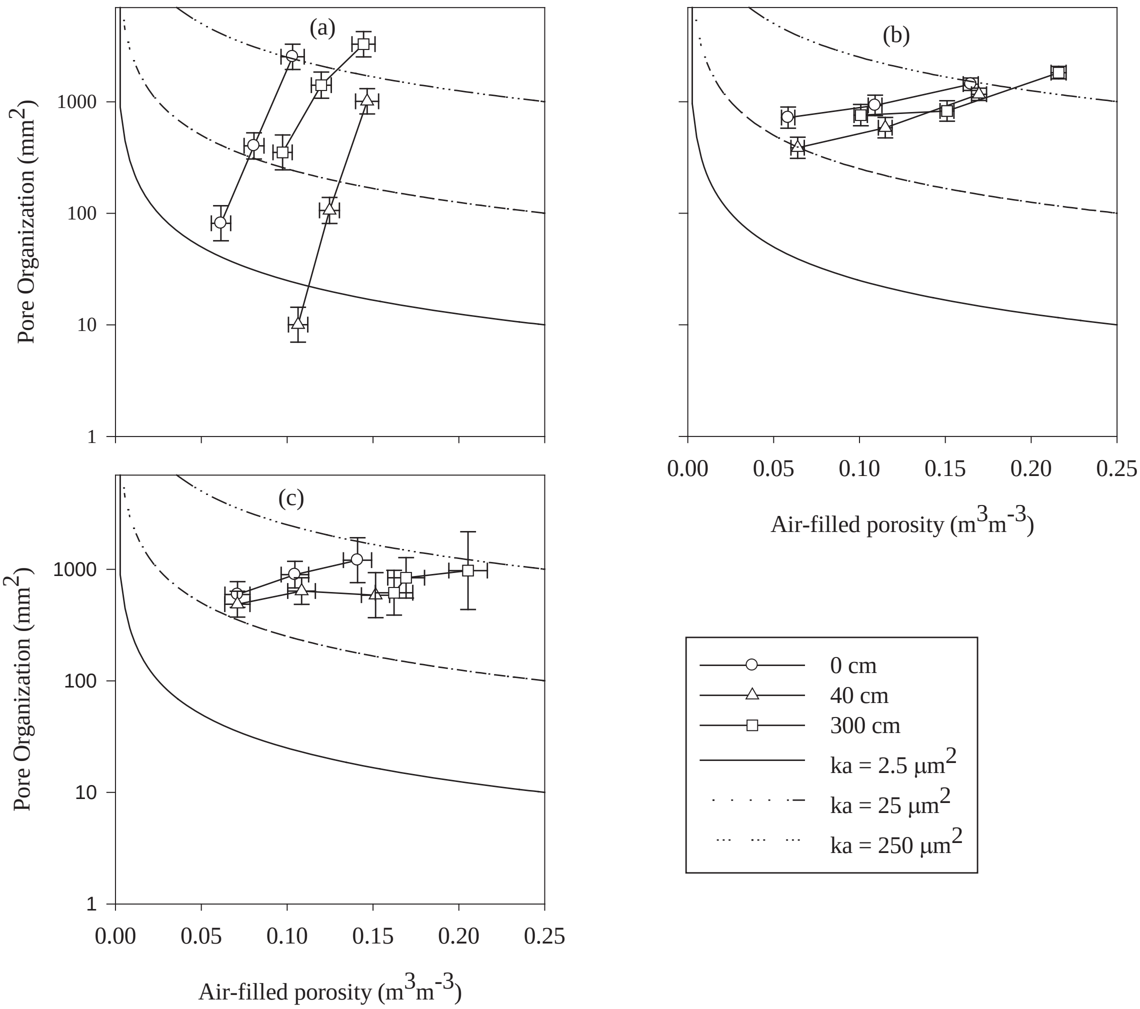

Figure 3. Pore organization as a function of air-filled porosity sampled at the center (circles), at the periphery (triangles), and outside (control; squares) of the wheel rut at 0.1 (a), 0.3(b), and 0.5 (c) m depth.

When soil drains, an increase in k_a can be attributed solely to an increase in ε_a or it can be attribute, in part, to other connectivity aspect of ε_a (*PO* could be regarded as one of the connectivity aspects). We can distinguish between these two possible ways by inspecting the evolution of k_a with *PO* and ε_a in Fig. 3. At 30 and 50 cm depth, all values for *PO* lie in the region between ka=25 and 250 µm^2. This implies that an increase in k_a was smaller than one order of magnitude across three matric potentials and it occurred most probably due to an increase in ε_a rather than an increase in *PO*. In contrast, for soils at 10 cm depth an increase in k_a was caused by increases both in *PO* and ε_a, as can be seen from Fig. 3a. At this depth, plots for each matric potentials were found to lie in different regions of k_a isolines, which implies an increase in k_a higher than an order of magnitude between two consecutive matric potentials.

Conclusion

The impact of traffic-induced changes on soil physical properties is usually quantified by collecting soil samples randomly in a trafficked area. This is tantamount to assuming that the vehicle pass would result in uniform changes in the soil physical properties within the wheel rut (soil-tyre contact area). This study produces strong evidence of inhomogeneous compaction effects across the wheel rut, which was pronounced especially at 10 cm depth: at the center of the wheel rut, both ea and ka reduced significantly, while at the periphery of the wheel rut only ka was significantly affected. We attribute this significant reduction in ka at the periphery of the wheel rut to shear damage. Our study shows that shear can produce great damage to soil structure and transport properties such as convective gas transport. Our sampling in a soil catena also provided better resolution on information about traffic induced changes on soil physical properties; this data may be useful for modeling purposes, where the assumption of a homogeneous compaction effect would be an inadequate oversimplification.

Acknowledgements

The technical assistance of Marlies Sommer (Agroscope ART) during field experimentation, sample collection and laboratory analyses is highly acknowledged. This work is part of a Scandinavian cooperation on the effects of subsoil compaction on soil functions (www.poseidon-nordic.dk). The study reported here was partly financed by the Danish Ministry of Food, Agriculture and Fisheries a. The PhD School SAFE of the Faculty of Agricultural Sciences at Aarhus University supported the PhD study of the first author

References

1. Gysi, M., Ott, A., Fluhler, H., 1999. Influence of single passes with high wheel load on a structured, unploughed sandy loam soil. Soil & Tillage Research 52, 141-151.
2. Richard, G., Cousin, I., Sillon, J.F., Bruand, A., Guérif, J., 2001. Effect of compaction on the porosity of a silty soil: influence on unsaturated hydraulic properties. European Journal of Soil Science 52, 49-58.
3. Berisso, F.E., Schjønning, P., Keller, T., Lamandé, M., Etana, A., de Jonge, L.W., Iversen, B.V., Arvidsson, J., Forkman, J., 2012. Persistent effects of subsoil compaction on pore size distribution and gas transport in a loamy soil. Soil and Tillage Research 122(0), 42-51.
4. Gupta, S.C., Hadas, A., Voorhees, W.B., Wolf, D., Larson, W.E., Schneider, E.C., 1985. Field testing of a soilcompactionmodel. In: Proceedings of the International Conference on Soil Dynamics, Auburn, AL, Vol. 5, pp. 979–994.
5. Keller, T., 2005. A Model for the Prediction of the Contact Area and the Distribution of Vertical Stress below Agricultural Tyres from Readily Available Tyre Parameters. Biosystems Engineering 92, 85-96.
6. O'Sullivan, M.F., Henshall, J.K., Dickson, J.W., 1999. A simplified method for estimating soil compaction. Soil and Tillage Research 49, 325-335.
7. Schjønning, P., Lamandé, M., Tøgersen, F.A., Arvidsson, J., Keller, T., 2008. Modelling effects of tyre inflation pressure on the stress distribution near the soil–tyre interface. Biosystems Engineering 99, 119-133.
8. Burt, E.C., Wood, R.K., Bailey, A.C., 1992. Some comparisons of average to peak soil-tire contact pressures. Transactions of the American Society of Agricultural Engineers 35, 401-404.
9. Gysi, M., 2001. Compaction of a Eutric Cambisol under heavy wheel traffic in Switzerland: - Field data and a critical state soil mechanics model approach. Soil and Tillage Research 61, 133-142.
10. Lamandé, M., Schjønning, P., 2008. The ability of agricultural tyres to distribute the wheel load at the soil–tyre interface. Journal of Terramechanics 45, 109-120.
11. Ball, B.C., Osullivan, M.F., Hunter, R., 1988. Gas-Diffusion, Fluid-Flow and Derived Pore Continuity Indexes in Relation to Vehicle Traffic and Tillage. Journal of Soil Science 39, 327-339.
12. Blackwell, P.S., Ringrosevoase, A.J., Jayawardane, N.S., Olsson, K.A., McKenzie, D.C., Mason, W.K., 1990. The use of air-filled porosity and intrinsic permeability to air to characterize structure of macropore space and saturated hydraulic conductivity of clay soils. Journal of Soil Science 41, 215-228.

13. Kenward, M.G., Roger, J.H., 1997. Small sample inference for fixed effects from restricted maximum likelihood. Biometrics 53, 983-997.
14. Berisso, F.E., Schjønning, P., Keller, T., Lamandé, M., Simojoki A., Iversen, B.V., Alakukku L., Forkman, J., 2012. Gas transport and subsoil pore characteristics: Anisotropy and long-term effects of compaction. Geoderma, In review.
15. Dörner, J., Horn, R., 2009. Direction-dependent behaviour of hydraulic and mechanical properties in structured soils under conventional and conservation tillage. Soil and Tillage Research 102, 225-232.
16. Peng, X.H., Horn, R., 2008. Time-dependent, anisotropic pore structure and soil strength in a 10-year period after intensive tractor wheeling under conservation and conventional tillage. Journal of Plant Nutrition and Soil Science-Zeitschrift Fur Pflanzenernahrung Und Bodenkunde 171, 936-944.
17. Schjønning, P., Munkholm, L.J., Moldrup, P., Jacobsen, O.H., 2002. Modelling soil pore characteristics from measurements of air exchange: the long-term effects of fertilization and crop rotation. European Journal of Soil Science 53, 331-339.